Archaea and bacteria with surprising microdiversity show shifts in dominance over 1,000-year time scales in hydrothermal chimneys

Q:1

William J. Brazelton[a,1], Kristin A. Ludwig[a,2], Mitchell L. Sogin[b], Ekaterina N. Andreishcheva[b], Deborah S. Kelley[a], Chuan-Chou Shen[c], R. Lawrence Edwards[d], and John A. Baross[a]

[a]School of Oceanography and Center for Astrobiology and Early Evolution, University of Washington, Seattle, WA 98195; [b]Josephine Bay Paul Center, Marine Biological Laboratory at Woods Hole, Woods Hole, MA 02543; [c]Department of Geosciences, National Taiwan University, Taipei 106, Taiwan; and [d]Department of Geology and Geophysics, University of Minnesota, Minneapolis, MN 55455

Edited by Rita R. Colwell, University of Maryland, College Park, MD, and approved December 11, 2009 (received for review May 18, 2009)

The Lost City Hydrothermal Field, an ultramafic-hosted system located 15 km west of the Mid-Atlantic Ridge, has experienced at least 30,000 years of hydrothermal activity. Previous studies have shown that its carbonate chimneys form by mixing of ~90 °C, pH 9–11 hydrothermal fluids and cold seawater. Flow of methane and hydrogen-rich hydrothermal fluids in the porous interior chimney walls supports archaeal biofilm communities dominated by a single phylotype of *Methanosarcinales*. In this study, we have extensively sampled the carbonate-hosted archaeal and bacterial communities by obtaining sequences of >200,000 amplicons of the 16S rRNA V6 region and correlated the results with isotopic (^{230}Th) ages of the chimneys over a 1,200-year period. Rare sequences in young chimneys were often more abundant in older chimneys, indicating that members of the rare biosphere can become dominant members of the ecosystem when environmental conditions change. These results suggest that a long history of selection over many cycles of chimney growth has resulted in numerous closely related species at Lost City, each of which is preadapted to a particular set of reoccurring environmental conditions. Because of the unique characteristics of the Lost City Hydrothermal Field, these data offer an unprecedented opportunity to study the dynamics of a microbial ecosystem's rare biosphere over a thousand-year time scale.

Q:2 biofilm | preadaptation | rare biosphere

Mucilaginous biofilms coat the porous carbonate mineral matrix of actively venting chimneys of the Lost City Hydrothermal Field (LCHF), an ultramafic-hosted system located 15 km west of the spreading axis of the Mid-Atlantic Ridge at a depth of ~750 m (1). Previous studies have shown that the biofilms contain 10^6–10^9 cells per gram of carbonate mineral and that >80% of the cells belong to a single phylotype of archaea known as Lost City *Methanosarcinales* (LCMS) (2). It is presumed that the abundant LCMS cells have adapted to the ~90 °C, pH 9–11 fluids and that they use high concentrations of dissolved hydrogen (H_2) and methane (CH_4) in the vent fluids (3, 4), but their physiology is unknown. As chimneys become less active, changes in mineralogy and fluid chemistry cause other organisms to become abundant (5). For example, chimneys with very little visible hydrothermal venting do not contain the LCMS biofilm. Instead, a single phylotype belonging to the ANME-1 group of anaerobic methanotrophic archaea is the dominant archaeon (5). The outer walls of carbonate chimneys, where mineralogy and fluid chemistry can be substantially different compared with the chimney interiors (2, 6), harbor bacteria with high similarity to sulfur- and methane-oxidizers, but archaea are much more abundant in chimneys venting up to 90 °C, high pH fluid (2).

Unlike typical black smoker systems that are fueled by heat from underlying magmatic activity, hydrothermal flow at the LCHF is driven by cooling of ultramafic rocks and lesser gabbroic material that underlie the field (1). Fluid chemistry is governed by exothermic geochemical reactions in the subsurface known as serpentinization (1). These reactions commonly occur in ultramafic environments on Earth where water reacts with the mineral olivine, and they are expected to occur on other planetary bodies hosting aqueous fluids (7). Serpentinization of subsurface ultramafic minerals is one of the most likely sources of CH_4 on Mars (8). At the LCHF, serpentinization reactions produce alkaline (pH 9–11) fluids that are rich in calcium (up to 30 mmol/kg), low in metals, and have near-zero concentrations of CO_2 (1, 4, 6). Serpentinization also provides an abiogenic source of H_2 (14 mmol/kg), CH_4 (2 mmol/kg), and low-molecular-weight hydrocarbons (3, 4). The ability of Lost City–like environments to generate reduced organic compounds exothermically and abiotically makes them plausible settings for the origin and early evolution of life (9).

Lost City also differs from most magma-driven systems in that it is very long-lived (10). Carbon isotopic measurements indicate that venting has been ongoing for at least 30,000 years, with individual chimneys active for at least 300 years, and modeling results indicate the system could remain active for up to 1 million years (10). Therefore, conditions within Lost City chimneys could have been conducive to the growth of LCMS for tens or hundreds of thousands of years, and it is possible that it has remained the dominant member of the ecosystem throughout that time. To our knowledge, biology has no precedent for such a low diversity, long-lived ecosystem. Characterizations of microbial community dynamics with respect to time are typically performed within the context of habitat monitoring. Numerous studies have described seasonal changes of particular communities (11, 12), documented initial colonizations of substrates (13), and observed short-term responses to environmental changes (14, 15). The time scales of these studies are on the order of months or at most years, practical time periods for observational studies. No direct evidence exists for changes in microbial communities occurring over longer time scales.

Technological advances in nucleic acid sequencing (16) are increasing the sensitivity at which changes in microbial communities can be detected. Recent high-sensitivity surveys of diverse environmental samples including those from shallow and deep ocean waters (17), hydrothermal fluids (17, 18), arctic tundra (19), and various soils (19, 20) have revealed that the vast majority of a microbial

Author contributions: W.J.B., K.A.L., M.L.S., D.S.K., and J.A.B. designed research; W.J.B., K.A.L., E.N.A., C.-C.S., and R.L.E. performed research; W.J.B., K.A.L., E.N.A., C.-C.S., and R.L.E. analyzed data; and W.J.B., K.A.L., M.L.S., D.S.K., and J.A.B. wrote the paper . Q:3, 4

The authors declare no conflict of interest.

This article is a PNAS Direct Submission. Q:5

Data deposition: Tag sequences are available in the VAMPS database (http://vamps.mbl.edu), and in the NCBI Short Read Archive under accession number SRP000912. Q:6

[1]To whom correspondence should be addressed. E-mail: bbrazelton@gmail.com.

[2]Present address: Consortium for Ocean Leadership, Washington, DC 20005.

This article contains supporting information online at www.pnas.org.cgi/content/full/0905369107/DCSupplemental.

habitat's diversity is comprised by taxa present at very low abundances—so low that they were previously undetectable. The most abundant organisms represent only a fraction of the total diversity. The high diversity of rare sequences indicates that they have been evolving over long periods of time and that at least some of them belong to organisms that are preadapted to environmental conditions that have occurred in the past and may reoccur in the future. A fundamental prediction of the "Rare Biosphere" model (17) is that when environmental conditions change, some of these rare, preadapted taxa can rapidly exploit the new conditions, increase in abundance, and out-compete the once abundant organisms that were adapted to the past conditions. No studies have tested this prediction by examining a shift in species composition involving extremely rare taxa occurring during a known time interval.

The longevity and extremely low diversity of the LCHF carbonate chimneys provide a unique test of the Rare Biosphere model. In this study, we use pyrosequencing technology to generate an extensive sequence dataset of the 16S rRNA V6 region from four carbonate chimney samples collected from structures varying from a massive edifice venting 88 °C, high pH fluid to a small, inactive chimney bathed in seawater. We investigate whether these low diversity communities harbor highly diverse but rare species and attempt to correlate our biological data with chimney sample ages derived from coregistered ^{230}Th isotopic measurements. We show that rare sequences in young chimneys samples are often much more abundant in older samples, suggesting that organisms can remain rare for long time periods until environmental changes allow them to proliferate.

Results

^{230}Th Dating of Carbonate Chimney Samples. Uranium–thorium (^{238}U-^{234}U-^{230}Th-^{232}Th or U-Th or ^{230}Th) disequilibrium dating is a powerful geochronological tool used to date inorganic and biogenic materials ranging in age from modern to 600 kyr (21). In this study, four discrete chimney samples (Fig. 1) were dated using ^{230}Th age-dating techniques. Sample 1 (^{230}Th age = 34.3 ± 8.1 yr) was collected from a site known as Marker 3 or Poseidon where emitting fluids reach 88 °C (4). Samples 2 and 3 are from a flange named Marker C that is bathed by fluids exhibiting a temperature gradient of 9–70 °C because of mixing of hydrothermal fluids with ambient seawater. Samples 2 and 3 were located 20 cm apart (Fig. 1) but yielded very different ages (^{230}Th ages = 42.9 ± 23.3 yr and 128.4 ± 57.2 yr, respectively). Sample 4 (^{230}Th age = 1245 ± 257 yr) was collected from a chimney with no visible venting and contained coral polyps on its exterior, typical of inactive chimneys at the LCHF (6). Complete descriptions of the samples and the ^{230}Th age-dating technique are available in SI.

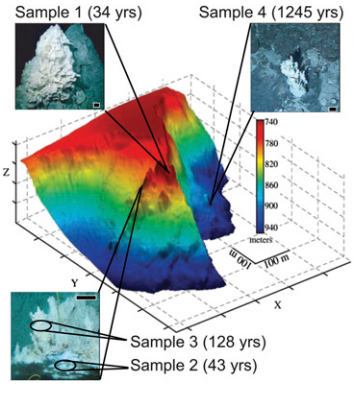

Fig. 1. Location within the Lost City Hydrothermal Field of carbonate chimney samples from which sequences were collected. Sample 1 was obtained from the pinnacle of the main edifice known as Poseidon, 50 m above the flange from which samples 2 and 3 were collected. Sample 4 is from a small, isolated chimney with no apparent venting activity found near the bottom of a cliff face. Scale bars in all photographs are 10 cm.

Archaeal Community Structure. Of 167,031 total archaeal V6 amplicons ("tags") sequenced from the four carbonate chimney samples (Fig. 1 and Table S1), we identified 2,635 unique sequence types that clustered into 817 operational taxonomic units (OTUs) at the 3% distance threshold. Sample 4 (^{230}Th age = 1245 ± 257 yr) contained significantly fewer OTUs than samples 1–3 (^{230}Th ages = 34–128 yr), as shown by the rarefaction curves of observed OTUs vs. the total number of tags sequenced (Fig. 2). The near-asymptotic shape of the rarefaction curves as well as the small difference between the observed numbers of OTUs and the values from two richness estimators (Table 1 and Table S1) indicate that our study has nearly completely sampled the archaeal V6 amplicon libraries from these samples.

Figure 3 presents normalized profiles of archaeal OTUs for each sample. A single OTU corresponding to the previously published 16S rRNA sequence of the putative methanogen Lost City *Methanosarcinales* (LCMS) (2, 5) comprised >90% of all tag sequences from samples 1–3. An additional 533 OTUs, none of which contained >5% of any sample's total tags, were also assigned to order *Methanosarcinales* (Fig. 3*B*) by the GAST automated taxonomic assignment process (22). The relative abundance of variant sequences generally decreased with increasing distance from the dominant sequence, a trend consistent with that expected from artificial diversity generated by pyrosequencing error. Several sequences occur much more frequently than predicted by random error, however, and probably represent genuine diversity. Furthermore, we have recently reported that variation in the V6 region of these *Methanosarcinales* sequences is correlated with greater variation in the intergenic transcribed spacer (ITS) region, a marker that often reflects physiological variation (23). Therefore, the number of OTUs measured in the V6 region by this study may underestimate the total genetic diversity.

The oldest sample (1245 ± 257 yr) was also dominated by a single OTU, but it corresponds to the previously published (5) 16S rRNA clone LC1133A-9, which is phylogenetically similar to the ANME-1 group of anaerobic methanotrophic archaea (Fig. 3*A*). Interestingly, the same OTU that dominates sample 4 is also present at low abundance in sample 1 (Fig. 3*B*), indicating that ANME-1 organisms are present in chimneys as young as 34 yr but are only dominant

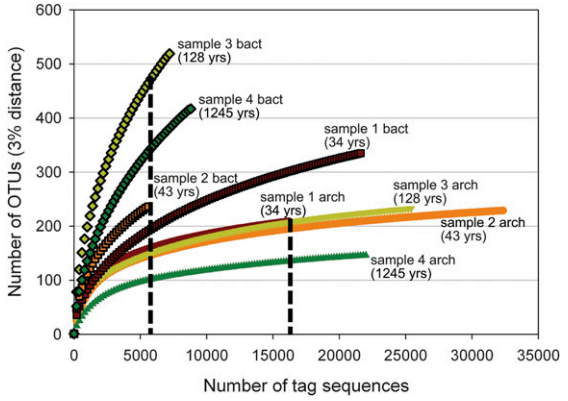

Fig. 2. Rarefaction analysis of archaeal and bacterial V6 tag sequences for each of the four chimney samples. OTUs, operational taxonomic units defined by clustering sequences with a 3% pairwise distance threshold. Bacterial diversity (curves outlined in black) is clearly greater than archaeal diversity in all samples. Rarefaction curves for archaeal sequences are near-asymptotic, indicating nearly complete sampling of archaeal V6 amplicon libraries. Dashed line indicates the point to which data were subsampled to compare diversity values among samples in Table 1.

Table 1. Comparison of ^{230}Th ages and V6 tag sequence diversity measurements for carbonate chimney samples from the Lost City Hydrothermal Field

			Archaea*				Bacteria*			
Chimney sample[†]	Max fluid temperature, °C	Age, yr	OTUs[‡]	ACE richness estimator[4]	Chao1 richness estimator[§]	Simpson's Reciprocal Index[§]	OTUs[‡]	ACE richness estimator[§]	Chao1 richness estimator[§]	Simpson's reciprocal index[§]
1	88	34.3 ± 8.1	342	448–568	441–599	2.04–2.13	177	283–388	217–319	5.6–5.9
2	70	42.9 ± 23.3	265	336–438	310–405	1.56–1.61	270	458–587	360–522	8.3–9.1
3	70	128.4 ± 57.2	265	322–410	301–386	1.64–1.69	428	859–1,061	648–925	20.0
4	Nd	1,245.4 ± 257.2	135	131–170	129–191	1.22–1.25	307	582–744	434–630	16.7

*Archaeal diversity is reported for OTU relative abundances normalized down to 16,260 tags; bacterial diversity is reported for OTU relative abundances normalized down to 5,567 tags. Table S1 compares both archaeal and bacteria diversity at 5,567 tags.
[†]DSV *Alvin* numbers for samples 1–4 are 3,881–1,408, 3,869–1,404, 3,869–1,443, and 3,876–1,133, respectively.
[‡]OTUs (operational taxonomic units) defined at 3% sequence difference.
[§]Ranges of diversity indices include 95% confidence intervals as calculated by DOTUR (39).

in much older chimneys. A third major archaeal group was represented by a set of sequences primarily present only in sample 1 and matching 16S rRNA clone LC1408cren-55, which is 97% similar over its full length to the ammonia-oxidizing crenarchaeon *Nitrosopumilus maritimus* (24). The presence of these sequences in the youngest, hottest chimney sample and, in hot chimney fluids (5), indicates that they probably represent thermophilic organisms, although their physiology is unclear because ammonia oxidation is not expected to be thermodynamically favorable in the anoxic fluids of LCHF chimneys.

The patterns visualized in Fig. 3 are quantified in two Venn diagrams illustrating the percentage of tags and numbers of OTUs shared among samples (Fig. S2). We also calculated overall community similarities (Fig. S3) based on the relative abundance of each OTU (Bray-Curtis similarity coefficient) as well as the presence/absence of each OTU (Jaccard similarity coefficient). As expected from Fig. 3, the three samples aged 34–128 yr were all very similar to each other (>85% Bray-Curtis, >48% Jaccard) and very different from sample 4 (<0.3% Bray-Curtis, <2% Jaccard). Remarkably, the archaeal community similarity between samples 2 and 3 (95% Bray-Curtis, 56% Jaccard) was much higher than the similarity between sample 1 replicates, so the small differences between samples 2 and 3 may not reflect any natural variation (additional details on estimation of variation between replicates in *SI Text*).

Bacterial Community Structure. Our study identified most of the diversity present in the bacterial V6 amplicon library from the youngest chimney sample (34.3 ± 8.1 yr), as shown by the nearly asymptotic rarefaction curve of OTUs discovered in sample 1 (Fig. 2). The rarefaction curves of samples 3 and 4 (128.4 ± 57.2 and 1245 ± 257 yr), in contrast, have very steep slopes and are therefore likely to contain much more diversity than we were able to discover with >7000 tag sequences from each sample. A few, highly abundant sequence types dominated the bacterial communities in each sample with rare sequences accounting for most of the observed diversity (Fig. 4). This pattern is very similar to that seen with the archaeal communities (Fig. 3*B*), although the bacterial communities have a more even distribution (reflected in the much higher Simpson's reciprocal index of diversity, Table 1 and Table S1) and have greater diversity, especially at large taxonomic distances (Fig. S1).

The taxonomic groups to which V6 tag sequences were assigned (Fig. 4) were consistent with previous work using different techniques (5). Notably, sequences assigned to *Gammaproteobacteria*, *Alphaproteobacteria*, *Firmicutes*, and *Chloroflexi* were the most abundant and diverse. The most abundant phylotypes in each group (Table S3) probably represent nonphotosynthetic organisms oxidizing reduced sulfur species (e.g., *Thiotrichales*, *Rhodobacterales*) or H_2 (e.g., *Clostridia*, *Dehalococcoidetes*) from the vent fluids. The small but significant quantities of abiotically-derived organic carbon found in Lost City hydrothermal fluids (4) may be an important carbon source for some of the bacteria, particularly *Clostridia* with high sequence similarity to *Desulfotomaculum* species, which occur in the youngest, most hydrothermally influenced sample (Table S3). Many *Clostridia* use low-molecular-

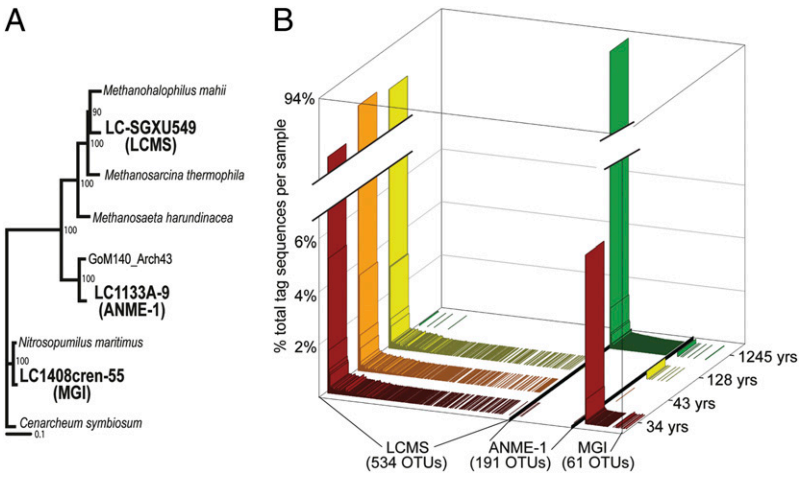

Fig. 3. Relative abundance distribution of archaeal OTUs among samples. (*A*) Bootstrapped phylogenetic tree of full-length archaeal 16S rRNA clones showing the relationship of three Lost City clones (in bold) to previously published close relatives. (*B*) Relative normalized abundance (as percentage of total tag sequences per sample) of each archaeal OTU (clustered at 3% distance threshold) in each of the four chimney samples. The OTUs are labeled according to which of the three groups they belong according to pairwise similarity with the V6 region of the full-length 16S rRNA clones. ANME-1, anaerobic methanotrophic archaea; LCMS, Lost City *Methanosarcinales*; MGI, Marine Group I *Crenarchaeota*.

weight organic acids, often in syntrophic association with methanogens (25–27). The possible ecological roles of these organisms in LCHF chimneys have been discussed previously (5).

Although the shifts in bacterial OTU composition are not as obvious as those in the archaeal communities, there are clear differences among samples with different ages (Fig. 4). Samples 1 and 2 (34.3 ± 8.1 and 42.9 ± 23.3 yr) have high overall community similarity (45% Bray-Curtis, 23% Jaccard), and samples 3 and 4 (128.4 ± 57.2 yr and 1245 ± 257 yr) are very similar to each other (34% Bray-Curtis, 23% Jaccard; Fig. S3). Note that samples 2 and 3, which were only ~20 cm apart in situ (Fig. 1) and had nearly identical archaeal communities, have only moderate bacterial community similarity (18% Bray-Curtis, 17% Jaccard). Interestingly, the distribution of OTUs among samples was roughly constant regardless of whether all OTUs are included in the analysis or if only abundant or if only rare OTUs are considered (Figs. S4 and S5). In short, samples of similar ages contain similar bacterial communities; with few exceptions, this trend is true for dominant as well as rare organisms.

Diversity Within *Thiomicrospira*. Previous work has shown that sequences most closely related to genus *Thiomicrospira* (order Thiotrichales; Table S3) are widely distributed throughout the LCHF (5). A single OTU assigned to genus *Thiomicrospira* corresponding to previously published full-length 16S rRNA clone LC1537B-12 comprised 37% of all bacterial V6 tags from the youngest sample (34.3 ± 8.1 yr). The same OTU also occurred in the other three samples but at lower relative abundance (28% at 43 yr, 3% at 128 yr, and 8% at 1,245 yr). An additional 23 OTUs (group C in Fig. 5), none of which comprised more than 2% of any sample's total tags, were at least 93% similar to clone LC1537B-12. Similarly, group A contained two dominant and several rare OTUs, all of which were at least 96.7% similar to the V6 region of clone LC1537B-49. The high occurrence of these OTUs in the younger, higher pH samples and absence in the two older, more neutral pH samples is consistent with the physiology of their closest relative (Fig. 5*A*), the alkaliphile *Thioalkalimicrobium cyclicum* (28). Group B OTUs, in contrast, were the most dominant *Thiomicrospira*-like sequences in sample 4, which showed no signs of venting and was likely the same temperature as the background seawater. All of these OTUs were at least 95% similar to a clone with 95.3% similarity over the full gene length to the pyschrophile *Thiomicrospira psychrophila* (29).

Although all samples have several *Thiomicrospira* OTUs, samples of different ages are dominated by different OTUs (Fig. 5). The most abundant *Thiomicrospira* OTU in the oldest sample, for example, is extremely rare in the youngest sample, and the overall similarity of the *Thiomicrospira* community between these two samples is low (24% Bray-Curtis, 22% Jaccard). As seen with the whole bacterial community, the two youngest samples have the most similar *Thiomicrospira* OTUs (61% Bray-Curtis, 32% Jaccard), and the two oldest samples are also very similar (39% Bray-Curtis, 31% Jaccard).

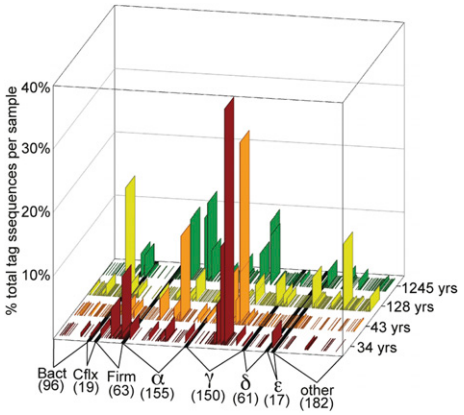

Fig. 4. Relative abundance distribution of bacterial OTUs among samples. OTUs are labeled according to their taxonomic assignment by the GAST process (22). α, *Alphaproteobacteria*; Bact, *Bacteroides*; Cflx, *Chloroflexus*; δ, *Deltaproteobacteria*; ε, *Epsilonproteobacteria*; Firm, *Firmicutes*; γ, *Gammaproteobacteria*.

Discussion

Dominance by a Few Species. Over the past >30,000 years of venting at the Lost City Hydrothermal Field (10), extreme environmental conditions created by mixing of <150 °C, pH 11 fluids enriched in dissolved H_2 and CH_4 with oxygen-rich seawater have selected for an unusual assemblage of microorganisms. Previous studies have shown that >80% of detectable cells in the warm, anoxic interior zones of carbonate chimneys are dominated by biofilms formed by Lost City *Methanosarcinales* (LCMS, 2). This study highlights the extremely low archaeal diversity of Lost City chimneys: >90% of all V6 tags in each sample clustered into a single OTU. Such extreme dominance of single phylotypes within hydrothermal chimneys is unprecedented; in other hydrothermal environments where methanogens dominate, diverse species adapted to various metabolic substrates are typically present (30, 31).

A small number of species also dominate the bacterial communities, and the identity of the dominant species often differs among chimney samples (Fig. 4). This trend is true even within narrow taxonomic groups. For example, chimney samples varied with respect to which OTUs representing genus *Thiomicrospira* dominated the community (Fig. 5). These organisms probably require reduced sulfur species from hydrothermal fluid, but they also need access to oxygen (the electron acceptor for all known *Thiomicrospira*) from seawater. Inorganic carbon is unavailable from high pH hydrothermal fluid, so organisms in chimneys with little exposure to seawater may be carbon-limited, as evidenced by the unprecedented enrichment of ^{13}C in lipids extracted from Lost City chimneys (32). Thus the diversity of *Thiomicrospira* sequences detected in this study (Fig. 5) probably resulted from many similar species adapting to slightly different niches within concentration gradients of reduced sulfur species, oxygen, and inorganic carbon as well as the associated temperature and pH gradients.

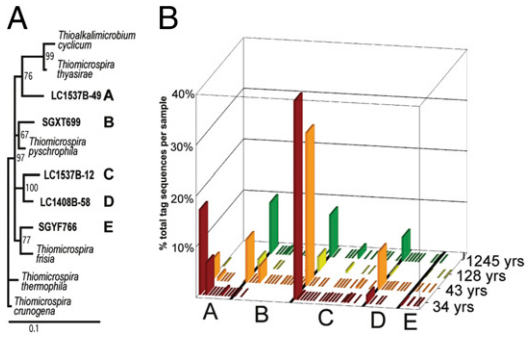

Fig. 5. Relative abundance distribution of *Thiomicrospira*-related OTUs among samples. (*A*) Bootstrapped phylogenetic tree of full-length 16S rRNA clones showing the relationship of Lost City clones (in bold) to previously published *Thiomicrospira* clones. (*B*) Relative normalized abundance of each OTU assigned to genus *Thiomicrospira* by GAST (22) in each of the four chimney samples. Pairwise similarities between sequences representative of each OTU and the V6 region of each clone were calculated, and OTUs were grouped according to which clone they were most closely related, as indicated by A–E labels. In groups A–D, similarities between sequences and clones ranged from 93 to 100%; in group E, 86–100%. OTUs within each group that have the highest similarity to the clone are sorted to the left.

Species Shift Between Rare and Dominant. The most notable differences in the archaeal community involve the shift to a community completely dominated by ANME-1 sequences in sample 4 (1245 ± 257 yr) as well as the relative lack of the Marine Group I *Crenarchaeota* in samples 2–4. Although ANME-1 sequences are nearly absent from samples 1–3, the identical sequence that dominates sample 4 is present, but rare, in sample 1 (34.3 ± 8.1 yr), which was collected from a chimney 100 m distant and shallower in depth. Deeper sequencing of samples 2 and 3 would most likely also recover this sequence at low abundance. Previous work has shown that ANME-1 sequences are present in multiple chimneys throughout the LCHF (5) including one chimney that has been dated to 10,500 years (33). Therefore, ANME-1 organisms are well dispersed throughout the vent field but are able to thrive only in chimneys that are not venting high-temperature, high-pH fluids, conditions typical of old chimneys (6). It is likely that these chimneys previously vented high-temperature, high-pH fluids and were therefore inhabited by microbial communities more similar to that of the younger chimneys reported here.

Many more examples of sequences that are rare in young samples but abundant in older samples are evident in the bacterial V6 tag pyrosequences (Fig. S6). Taxonomic differences among chimney samples of varying ages are most likely caused by differences in mineralogy and fluid chemistry, and both of these factors are expected to change with somewhat predictable trends during the cycle of chimney formation, growth, and senescence (6). Although fluid chemistry is less directly correlated to chimney sample age than mineralogy, it is clear, that over long time scales, fluid chemistry strongly determines the mineralogy of chimneys (6). On short time scales, fluctuations in chemistry may affect microbial communities independently of mineralogy and chimney sample age, and it can be expected that these factors will have varying influences on different organisms.

Further work is necessary to confidently distinguish the influences of mineralogy, fluid chemistry, and age on each archaeal and bacterial species; but in general our results show that chimney sample age can be a useful indicator of bacterial community composition (Fig. 4). For example, samples 2 and 3 were collected from the same chimney flange, separated by ≈20 cm in situ, but have remarkably different bacterial communities (18% Bray-Curtis similarity). Sample 2 (42.9 ± 23.3 yr) was closer to the vent flange opening and is composed of aragonite ($CaCO_3$) and brucite ($Mg(OH)_2$) minerals that are stable in vent fluid–dominated environments. In contrast, sample 3 is older (128.4 ± 57.2 yr), contains more calcite than aragonite (calcite is a polymorph of metastable aragonite) and little brucite, and was more exposed to ambient seawater (6). Clearly, the distribution of bacterial species correlates more strongly with sample age and mineralogy than with physical distance, as sample 2 has high similarity (45% Bray-Curtis) with sample 1, which is from a different chimney but of similar mineralogy and age (34.3 ± 8.1 yr). Moreover, sample 3 is dominated by the same bacterial sequences as sample 4 (1245 ± 257 yr), even though those two samples were separated by at least 100 m laterally and in depth. The four samples examined in this study do not constitute strong statistical evidence, but the initial data from this study, together with previous surveys of microbial diversity and geochemistry of additional samples (5, 6), are consistent with a correlation of mineralogy and age with microbial community composition.

The archaeal communities, in contrast, appear to be more strongly influenced by fluid chemistry when comparing samples younger than ~150 yr. Although samples 2 and 3 have different ages and bacterial communities, their archaeal populations are practically identical (95% Bray-Curtis similarity). Both samples were exposed to the same hydrothermal fluid, which may have fueled the same archaeal population while bacteria in the older sample adapted over time to the increased influence of cold seawater that also resulted in mineralogical and porosity changes (6). Both samples have high cell densities and high proportions of archaea (Table S4), indicating that the archaeal populations are strongly stimulated by the conditions at this chimney flange. Thus, the archaeal community may not be influenced by mineralogical changes as long as fluid chemistry (e.g., H_2 and CH_4 concentrations) remains constant. Indeed, minor differences in fluid chemistry (3, 4) between chimneys may explain the presence of *Crenarchaeota* in sample 1 but not sample 2, which is of nearly identical age (Table 1).

The Lost City Rare Biosphere. The archaeal and bacterial communities inhabiting carbonate chimneys at the LCHF are not "frozen in time" and do not record the history of the chimneys. Nevertheless, many chimneys must have formed, grown, and become inactive during the >30,000 years that the LCHF has been active (10). Furthermore, it is clear that mineralogy and fluid chemistry are correlated over long time scales with chimney growth stages (6) and chimney age (33). Therefore, we infer that old chimneys formerly had environmental characteristics typical of younger chimneys. There is no reason to expect important differences between young chimneys active today and young chimneys that were active thousands of years ago. If environmental conditions broadly determine microbial community composition, microbial communities inhabiting chimneys today should resemble those that inhabited chimneys of similar ages hundreds or thousands of years ago. Although we have been able to collect V6 tag pyrosequences from only four samples, previous studies of LCHF chimneys have shown that archaeal and bacterial communities change when chimneys become less active (5). Furthermore, ^{230}Th ages of additional LCHF chimney samples are consistent with the trend that chimney samples of similar ages have similar mineralogy and fluid chemistry (33). In conclusion, the results from this study and others (1, 5, 6, 10, 33) support a connection between microbial community composition and the geochemical conditions characteristic of a chimney sample's age over long time scales.

The shifts in community composition observed in this study do not reflect new speciation events. Our results show that organisms favorably selected by new conditions already existed at low levels before the environmental change occurred (Fig. S6). Therefore, the genomes of the favorably selected organisms must have already encoded the necessary adaptations before the change. They were preadapted to the new conditions. Alternatively, every community shift may have resulted from a rare organism acquiring a useful gene via lateral gene transfer. Another possibility is that mutation and/or recombination occurred much more quickly in genes required for the adaptation but not in the V6 hypervariable region measured in this study. These processes may occur, but a more parsimonious explanation of the many shifts detected in this study where a rare organism rapidly increased its relative abundance is that these organisms had been preadapted for hundreds or thousands of years to the particular niche created by the environmental change. Therefore, the rare biosphere of the Lost City microbial community represents a large repository of genetic memory created during a long history of past environmental changes that selected for new species within a small pool of organisms that originally colonized the extreme environment. The rare organisms were able to rapidly exploit new niches as they arose because they had been previously selected for the same conditions in the past.

The Lost City Hydrothermal Field has been active for at least 30,000 years and probably much longer (10). Ultramafic environments such as Lost City have surely existed throughout Earth's history and were probably much more widespread on the early Earth when ultramafic lavas were more common (1, 34). Indeed, the large quantities of hydrogen generated at ultramafic-hosted systems like Lost City may have supported the earliest ecosystems on Earth (35, 36). Therefore, the ecological dynamics described in this study may have been occurring in similar environments for most of Earth's history, and the large pool of rare organisms present today may reflect that long history.

Methods

Pyrosequencing and Diversity Calculations. Carbonate chimney samples were collected from the LCHF with DSV *Alvin* during cruise AT07-34 aboard the R/V *Atlantis* in April/May 2003 (http://www.lostcity.washington.edu). Detailed descriptions of ^{230}Th dating techniques and the DNA extraction protocol are available in *SI Text.* V6 amplicon libraries were constructed and sequenced as in refs. 17 and 18 with a 454 Life Sciences GS20 pyrosequencer and a 454 Life Sciences FLX pyrosequencer for the archaeal data. Tag sequences were screened for quality as recommend by (37). Archaeal and bacterial sequence alignments were constructed by submitting to the NAST aligner (http://greengenes.lbl.gov) all unique sequences pooled from all four samples, including primers to ensure full-length alignment. Obvious alignment errors were manually corrected, and primers were trimmed, resulting in final archaeal and bacterial alignments in which most sequences contained 60–65 bp. Similar results as those reported here were achieved by aligning with MUSCLE (38). The distance matrix for each alignment was calculated with quickdist as described elsewhere (17). Sequences were clustered into OTUs, and rarefaction curves and diversity estimators were calculated with DOTUR (39). Some of the rare sequences detected in this study may be artifacts of pyrosequencing technology (40, 41), but this possibility does not affect the main conclusions of our study. Because many of the rare sequences are much more abundant in other samples, these sequences are clearly not artifacts. Furthermore, we have recently reported that diversity in V6 tag pyrosequences is correlated to diversity at another marker and may actually underestimate the total genetic diversity (23). Additional methods for pyrosequencing and error determination are available in *SI Text.*

Comparison of OTU Membership Among Samples. After sequences were clustered into OTUs with DOTUR, the program SONS (42) was used to determine the relative abundance distribution of each OTU in each sample. The SONS output informed creation of the plots in Figs. 3–5 and Figs. S2–S6. Samples 1–4 yielded 16260, 32345, 25471, and 21983 archaeal tags and 21582, 5567, 7162, and 8716 bacterial tags, respectively. To normalize relative abundances of each OTU among samples, tags were randomly resampled down to the sample with the fewest tags using Daisy-Chopper (available from P. Swift, J. Gilbert, and D. Field) after clustering OTUs. Q:13 Consequently, normalized numbers of OTUs reported in Table 1 and Figs. 3–5 are lower than the total nonnormalized values reported in Table S1 and Fig. 2. Bray-Curtis and Jaccard similarities between samples were calculated with Primer 6 (http://www.primer-e.com) without any further data transformation. Taxonomies were assigned to each tag by the GAST process (22) via the VAMPS website.

Data Availability. All V6 sequence data are available at the VAMPS database (http://vamps.mbl.edu), under dataset names ICM_LCY_Av6 and ICM_LCY_Bv6 and in the NCBI Short Read Archive under submission number SRP000912. See Supplementary Information for sample names in the databases.

ACKNOWLEDGMENTS. We express our appreciation to the crews of the R/V *Atlantis* and DSV *Alvin* and the scientific party of the 2003 Lost City Expedition. We thank J. Huber and S. Huse for helpful discussions. This research was supported by the W.M. Keck Foundation to M.L.S., the NASA Astrobiology Institute through the Carnegie Institution for Science to J.A.B. and through the MBL to M.L.S., NSF Grant OCE0137206 and NOAA Ocean Exploration support to D.S.K., and Grants 96-2116-M002-003 and 97-2752-M004-PAE to C.-C.S. Q:14

1. Kelley DS, et al. (2005) A serpentinite-hosted ecosystem: The Lost City hydrothermal field. *Science* 307:1428–1434.
2. Schrenk MO, Kelley DS, Bolton SA, Baross JA (2004) Low archaeal diversity linked to subseafloor geochemical processes at the Lost City Hydrothermal Field, Mid-Atlantic Ridge. *Environ Microbiol* 6:1086–1095.
3. Proskurowski G, Lilley MD, Kelley DS, Olson EJ (2006) Low temperature volatile production at the Lost City Hydrothermal Field, evidence from a hydrogen stable isotope geothermometer. *Chem Geol* 229:331–343.
4. Proskurowski G, et al. (2008) Abiogenic hydrocarbon production at Lost City Hydrothermal Field. *Science* 319:604–607.
5. Brazelton WJ, Schrenk MO, Kelley DS, Baross JA (2006) Methane- and sulfur-metabolizing microbial communities dominate the Lost City Hydrothermal Field ecosystem. *Appl Environ Microbiol* 72:6257–6270.
6. Ludwig KA, Kelley DS, Butterfield DA, Nelson BK, Früh-Green G (2006) Formation and evolution of carbonate chimneys at the Lost City Hydrothermal Field. *Geochim Cosmochim Acta* 70:3625–3645.
7. Schulte M, Blake D, Hoehler T, McCollom T (2006) Serpentinization and its implications for life on the early Earth and Mars. *Astrobiology* 6:364–376.
8. Oze C, Sharma M (2005) Have olivine, will gas: Serpentinization and the abiogenic production of methane on Mars. *Geophys Res Lett* 32:L10203.
9. Martin W, Baross J, Kelley D, Russell MJ (2008) Hydrothermal vents and the origin of life. *Nat Rev Microbiol* 6:805–814.
10. Früh-Green GL, et al. (2003) 30,000 Years of hydrothermal activity at the Lost City Vent Field. *Science* 301:495–498.
11. Dimitriu PA, Pinkart HC, Peyton BM, Mormile MR (2008) Spatial and temporal patterns in the microbial diversity of a meromictic soda lake in Washington State. *Appl Environ Microbiol* 74:4877–4888.
12. Moisander PH, Morrison AE, Ward BB, Jenkins BD, Zehr JP (2007) Spatial-temporal variability in diazotroph assemblages in Chesapeake Bay using an oligonucleotide nifH microarray. *Environ Microbiol* 9:1823–1835.
13. Pagé A, Tivey MK, Stakes DS, Reysenbach A-L (2008) Temporal and spatial archaeal colonization of hydrothermal vent deposits. *Environ Microbiol* 10:874–884.
14. Goffredi SK, Wilpiszeski R, Lee R, Orphan VJ (2008) Temporal evolution of methane cycling and phylogenetic diversity of archaea in sediments from a deep-sea whale-fall in Monterey Canyon, California. *ISME J* 2:204–220.
15. Lear G, Anderson MJ, Smith JP, Boxen K, Lewis GD (2008) Spatial and temporal heterogeneity of the bacterial communities in stream epilithic biofilms. *FEMS Microbiol Ecol* 65:463–473.
16. Margulies M, et al. (2005) Genome sequencing in microfabricated high-density picolitre reactors. *Nature* 437:376–380.
17. Sogin ML, et al. (2006) Microbial diversity in the deep sea and the underexplored "rare biosphere". *Proc Natl Acad Sci USA* 103:12115–12120.
18. Huber JA, et al. (2007) Microbial population structures in the deep marine biosphere. *Science* 5:97–100.
19. Neufeld JD, Li J, Mohn WW (2008) Scratching the surface of the rare biosphere with ribosomal sequence tag primers. *FEMS Microbiol Lett* 283:146–153.
20. Roesch LFW, et al. (2007) Pyrosequencing enumerates and contrasts soil microbial diversity. *ISME J* 1:283–290.
21. Edwards RL, Chen JH, Wasserburg GJ (1986/1987) ^{238}U -^{234}U-^{230}Th-^{232}Th systematics and the precise measurement of time over the past 500,000 years. *Earth Planet Sci Lett* 81:175–192.
22. Huse SM, et al. (2008) Exploring microbial diversity and taxonomy using SSU rRNA hypervariable tag sequencing. *PLoS Genet* 4:e1000255.
23. Brazelton WJ, Sogin ML, Baross JA (2009) Multiple scales of diversification within natural populations of archaea in hydrothermal chimney biofilms. *Environ Microbiol Reports* DOI: Q:15 10.1111/j.1758-2229.2009.00097.x.
24. Könneke M, et al. (2005) Isolation of an autotrophic ammonia-oxidizing marine archaeon. *Nature* 437:543–546.
25. Cao XH, Liu XL, Dong XZ (2003) *Alkaliphilus crotonatoxidans* sp. nov., a strictly anaerobic, crotonate-dismutating bacterium isolated from a methanogenic environment. *Int J Syst Evol Microbiol* 53:971–975.
26. Imachi H, et al. (2006) Non-sulfate-reducing, syntrophic bacteria affiliated with *desulfotomaculum* cluster I are widely distributed in methanogenic environments. *Appl Environ Microbiol* 72:2080–2091.
27. Lueders T, Pommerenke B, Friedrich MW (2004) Stable-isotope probing of microorganisms thriving at thermodynamic limits: Syntrophic propionate oxidation in flooded soil. *Appl Environ Microbiol* 70:5778–5786.
28. Sorokin DY, et al. (2002) *Thioalkalimicrobium cyclicum* sp. nov. and *Thioalkalivibrio jannaschii* sp. nov., novel species of haloalkaliphilic, obligately chemolithoautotrophic sulfur-oxidizing bacteria from hypersaline alkaline Mono Lake (California). *Int J Syst Evol Microbiol* 52:913–920.
29. Knittel K, et al. (2005) *Thiomicrospira arctica* sp. nov. and *Thiomicrospira psychrophila* sp. nov., psychrophilic, obligately chemolithoautotrophic, sulfur-oxidizing bacteria isolated from marine Arctic sediments. *Int J Syst Evol Microbiol* 55:781–786.
30. Dhillon A, et al. (2005) Methanogen diversity evidenced by molecular characterization of methyl coenzyme M reductase A (mcrA) genes in hydrothermal sediments of the Guaymas Basin. *Appl Environ Microbiol* 71:4592–4601.
31. Nercessian O, Bienvenu N, Moreira D, Prieur D, Jeanthon C (2005) Diversity of functional genes of methanogens, methanotrophs and sulfate reducers in deep-sea hydrothermal environments. *Environ Microbiol* 7:118–132.
32. Bradley AS, Hayes JM, Summons RE (2009) Extraordinary ^{13}C enrichment of diether lipids at the Lost City Hydrothermal Field indicates a carbon-limited ecosystem. *Geochim Cosmochim Acta* 73:102–118.
33. Ludwig KA, Shen C, Kelley DS, Cheng H, Edwards R (2009) U-Th isotopic systematics and ages of carbonate chimneys at the Lost City Hydrothermal Field, *Eos Trans AGU*, 90(Suppl):Abstract V31D-2007. Q:16
34. Grove TL, Parman SW (2004) Thermal evolution of the Earth as recorded by komatiites. *Earth Planet Sci Lett* 219:173–187.
35. Nesbet EG, Sleep NH (2001) The habitat and nature of early life. *Nature* 409: 1082–1091.
36. Olson JM (2006) Photosynthesis in the Archean era. *Photosynth Res* 88:109–117.
37. Huse SM, Huber JA, Morrison HG, Sogin ML, Welch DM (2007) Accuracy and quality of massively parallel DNA pyrosequencing. *Genome Biol* 8:R143. Q:17
38. Edgar RC (2004) MUSCLE: Multiple sequence alignment with high accuracy and high throughput. *Nucleic Acids Res* 32:1792–1797.
39. Schloss PD, Handelsman J (2005) Introducing DOTUR, a computer program for defining operational taxonomic units and estimating species richness. *Appl Environ Microbiol* 71:1501–1506.
40. Quince C, et al. (2009) Accurate determination of microbial diversity from 454 pyrosequencing data. *Nat Methods* 6:639–641.
41. Kunin V, Engelbrektson A, Ochman H, Hugenholtz P (2009) Wrinkles in the rare biosphere: Pyrosequencing errors lead to artificial inflation of diversity estimates. *Environ Microbiol* 10.1111/j.1462-2920.2009.02051.x. Q:18
42. Schloss PD, Handelsman J (2006) Introducing SONS, a tool for operational taxonomic unit-based comparisons of microbial community memberships and structures. *Appl Environ Microbiol* 72:6773–6779.

AUTHOR QUERIES

AUTHOR PLEASE ANSWER ALL QUERIES 1

Q: 1_Please contact PNAS_Specialist@dartmouthjournals.com if you have questions about the editorial changes, this list of queries, or the figures in your article. Please include your manuscript number in the subject line of all e-mail correspondence; your manuscript number is 200905369. Please (i) review the author affiliation and footnote symbols carefully, (ii) check the order of the author names, and (iii) check the spelling of all author names and affiliations. Please indicate that the author and affiliation lines are correct by adding the comment "OK" next to the author line. Please note that this is your opportunity to correct errors in your article prior to publication. Corrections requested after online publication will be considered and processed as errata.

Q: 2_PNAS allows up to five key terms that (i) do not repeat terms present in the title (which is searchable online) and (ii) do not include nonstandard abbreviations. You may add two terms. Also, please check the order of your key terms and approve or reorder them as necessary.

Q: 3_Please review the information in the author contribution footnote carefully. Please make sure that the information is correct and that the correct author initials are listed. Note that the order of author initials matches the order of the author line per journal style. You may add contributions to the list in the footnote; however, funding should not be an author's only contribution to the work.

Q: 4_You will receive a notification from the PNAS eBill system in 1-2 days. Each corresponding author is required to log in to the system and provide payment information for applicable publication charges (purchase order number or credit card information) upon receipt of the notification. You will have the opportunity to order reprints through the eBill system if desired, as well. Failure to log in and provide the required information may result in publication delays.

Q: 5_Reminder: You have chosen not to pay an additional $1275 (or $950 if your institution has a site license) for the PNAS Open Access option.

Q: 6_Please make sure that the sequences are released by GenBank or another publicly accessible database before your page proofs are returned. It is PNAS policy that the data be released BEFORE the paper can appear in print.

Q: 7_Please advise whether "Marker" may be changed to "marker" throughout in keeping with journal style, which typically lower cases designative terms.

Q: 8_Please verify that all supporting information (SI) citations are correct. Note, however, that the hyperlinks for SI citations will not work until the article is published online. In addition, SI that is not composed in the main SI PDF (appendices, datasets, movies, and "Other Supporting Information Files") have not been changed from your originally submitted file and so are not included in this set of proofs. The proofs for any composed portion of your SI are included in this proof as subsequent pages following the last page of the main text. If you did not receive the proofs for your SI, please contact **PNAS_Specialist@dartmouthjournals.com**.

Q: 9_Please cite Fig. 3*A* before Fig. 3*B* if possible.

AUTHOR QUERIES

AUTHOR PLEASE ANSWER ALL QUERIES 2

Q: 10_SI figures must be cited in order in the main text. Please cite Fig. S1 before Fig. S2.

Q: 11_Please cite Table S2 before Table S3.

Q: 12_Please cite Figs. S4 and S5 before Fig. S6

Q: 13_Please clarify Swift, Gilbert, and Field source.

Q: 14_Please spell out NASA, MBL, NSF, and NOAA

Q: 15_Please update reference 23 publication information.

Q: 16_Please replace Ref. 33 with full article if possible, as abstracts are not permitted in the reference list. If this must be included as is, please place the information in a footnote to the text and renumber the remaining references and citations accordingly.

Q: 17_Reference has only first page number. Please provide the last page number if article is longer than one page. (in reference 37 "Huse, Huber, Morrison, Sogin, Welch, 2007").

Q: 18_Please update publication information for reference 41.

Supporting Information

Brazelton et al. 10.1073/pnas.0905369107

SI Methods

Sample Names. Samples 1–4 in this study refer to DSV *Alvin* sample names 3,881–1,408, 3,869–1,404, 3,869–1,443, and 3,876–1,133, respectively. The NCBI Short Read Archive and names of 16S rRNA clones from previous studies (2) refer to samples 1–4 as LC1408, LC1404, LC1443, and LC1133, respectively. The VAMPS database (http://vamps.mbl.edu) identifies archaeal V6 tag sequences from this study as ICM_LCY_Av6 and bacterial V6 tag sequences as ICM_LCY_Bv6. Samples 1–4 are designated in VAMPS as LCY_0016_2003_05_16, LCY_0014_2003_05_04, LCY_0018_2003_05_04, and LCY_0012_2003_05_11, respectively, and bacterial V6 tag sequences as LCY_0005_2003_05_16, LCY_0003_2003_05_04, LCY_0007_2003_05_04, and LCY_0001_2003_05_11, respectively.

Sample Descriptions. Previous studies have used field observations to classify the LCHF chimney samples based on observable hydrothermal activity (where "active" samples are those egressing hydrothermal fluids and "inactive" chimneys have no apparent venting activity) (5). Active structures are typically very friable, porous (up to 50%) and are composed of a mix of aragonite ($CaCO_3$), brucite ($Mg(OH)_2$), and some calcite ($CaCO_3$) whereas inactive samples are typically more lithified and are composed of mostly aragonite and calcite (5). In this study, three samples from actively venting chimneys (samples 1–3) and one sample from an inactive chimney (sample 4) were selected to obtain a set of samples ranging from young to old and ranging from close to distant physical proximity. All samples were collected with DSV *Alvin* and stored in a closed "biobox" until shipboard retrieval. Samples 2 and 3 were collected on the same dive; other samples were collected on separate dives. Previously published microbiological and biochemical characteristics of these samples are summarized in Table S4.

Samples 2 (42.9 ± 23.3 yr) and 3 (128.4 ± 57.2 yr) are from a structure named "Marker C" and were located 20 cm apart (Fig. 1). Marker C is a ~50-cm-wide flange structure with several small (centimeters tall) chimneys growing on the top of the flange (Fig. 1). Sample 2 was collected from the front of the flange, and sample 3 was a small spire collected from the top (Fig. 1). Both structures were cream white with a reddish discoloration that remains unexplained (5). These chimneys were visibly venting, and the mixing of emitting fluids with ambient seawater created a temperature gradient of 9–70 °C from the interior of the flange outward. Porosity of the LCHF active chimneys ranges from <5% to 50% and is determined quantitatively using petrographic thin sections (5). Only one thin section of a sample in this study (sample 3) was made, which had a porosity of 33% (5). Samples representing earlier growth stages generally have higher porosities than samples representing later growth stages (5), so it is expected that samples 1–2 have >33% porosity, and sample 4 has <33% porosity. Visual examination of the samples supports this hypothesis, but quantitative measurements were not conducted.

Sample 1 (34.3 ± 8.1 yr) was collected from a site known as "Marker 3" or "Poseidon" (6). Poseidon is the landmark of the LCHF, towering 60 m above the seafloor, emitting fluids at temperatures of 55–88°C. Sample 1 minerals appeared bright white in color, very friable, and not lithified. A mucilaginous substance, most likely a biofilm, coated the sample.

Sample 4 (1,245 ± 257.2 yr) was collected from a small spire growing from the basement rock on the eastern side of the field (Fig. 1). This structure was not visibly venting, although it was observed only once before sampling. It was gray in color, contained some biolithic material and had visible fluid flow channels, suggesting that some venting may have occurred in the recent past. Coral polyps were found on the exterior of the structure after recovery, which is typical of inactive chimneys at the LCHF (5). Temperature and chemistry conditions at this site were presumed to be that of ambient seawater, and no measurements were performed.

Fluid chemistry and temperature data from the chimneys at Marker 3 (sample 1) and Marker C (samples 2–3) do not shown any obviously important differences (7, 8). The chimney at Marker 3 appears slightly hotter (88 °C maximum temperature compared with 70 °C maximum temperature), but the in situ temperature of the minerals collected in this study would have been determined by their distance from the fluid source. Sample 3 was most likely at a much cooler temperature than sample 2 because it was further from the chimney flange opening. Concentrations of H_2 and carbon species are highly similar at markers 3 and C (7, 8). Chimney mineralogy and ^{230}Th age, therefore, are expected to be much more important drivers of microbial community composition than are temperature and fluid chemistry, and the data presented in this study is consistent with that hypothesis.

U/Th Dating of Carbonate Chimneys. Numerous questions remain concerning the development, formation conditions, and microbial colonization of this novel hydrothermal system. Although previous work using radiocarbon techniques shows that hydrothermal activity has been ongoing for at least 30 kyr, modeling suggests that the field may be even older (9). The carbonate composition of the LCHF chimneys (5, 6) is amenable to both radiocarbon and U-series dating, allowing important constraints to be placed on the history of hydrothermal activity and the timescales over which the chimneys form. Uranium–thorium (^{238}U-^{234}U-^{230}Th-^{232}Th or U-Th or ^{230}Th) disequilibrium dating is a powerful geochronological tool used to date inorganic and biogenic materials ranging in age from modern to 600 kyr (10–12). In this study, four discrete chimney samples were dated using ^{238}U-^{234}U-^{232}Th-^{230}Th age dating techniques to compare these ages to the microbial community structure of coregistered samples.

For U-Th shore-based analyses, chimney subsamples were chemically prepared in the Minnesota Isotope Lab (MIL) using methods described in Edwards et al. (10) and Shen et al. (13). Approximately 0.2 g of carbonate was weighed in acid-cleaned Teflon beakers, dissolved in HNO_3, then spiked, as described by Chen and Wasserburg (1981) and Chen et al. (14). After adding Q:1 5 drops of $HClO_4$, the samples were capped and heated for 4–6 h to remove organics and equilibrate the spike with the sample. Uranium and Th aliquots were separated using Fe coprecipitation and ion chromatography, dissolved in 1% HNO_3 + 0.005 N HF, and then stored in acid-cleaned plastic ICP vials. Procedural blanks were measured regularly. Three-month average values were 0.02 ± 0.01 pmol ^{238}U, 0.003 ± 0.003 pmol ^{232}Th, and 0.0006 ± 0.0005 fmol ^{230}Th.

All samples were analyzed on an ICP-SF-MS using methods described by Shen et al. (15). Data reduction was completed offline as described by Cheng et al. (16) and Shen et al. (15). Ages were calculated iteratively as described by Edwards et al. (11) and Shen et al. (15). Values for decay constants λ_{230} (9.1577×10^{-6} yr^{-1}) and λ_{234} (2.8263×10^{-6} yr^{-1}) are from Cheng et al. (16) and λ_{238} (1.5513×10^{-10} yr^{-1}) is from Jaffey et al. (17). Measured errors of isotopic and concentration are given as 2 standard deviations of the mean ($2\sigma_m$) and age precisions are reported as 2 standard deviations (2σ). Ages of subsamples from

the same large sample were highly similar (K. Ludwig doctoral dissertation; manuscript in preparation), indicating that ages of the four samples in this study are representative of the bulk material used for DNA extraction.

DNA Extraction from Carbonate Chimneys: Shipboard, subsamples of chimney material were frozen immediately at −80 °C and remained frozen until onshore analysis. DNA was extracted from carbonate chimney samples according to a protocol modified from previous reports (2, 18) and summarized here. After crushing a frozen carbonate sample with a sterile mortar and pestle, ≈0.25–0.5 g of chimney material were placed in a 2-mL microcentrifuge tube containing 250 μL of 2× buffer AE (200 mM Tris, 50 mM EDTA, 300 mM EGTA, 200 mM NaCl, pH 8) and 2 μg of poly-dIdC (Sigma-Aldrich) and incubated at 4 °C overnight to allow chelation of salts and binding of DNA to poly-dIdC. Between 36 and 72 replicate tubes were processed in parallel, and a ≈15-g quantity of carbonate minerals was processed for each sample. Proteinase K (final concentration 1.2 mg/mL) and 10 μL of 20% SDS were added to each tube before incubation at 37 °C for at most 30 min. An additional 150μL of 20% SDS and 500 μL of phenol:chloroform:isoamyl alcohol (25:24:1 ratio by volume) were added to each tube before centrifugation at 12,000 × *g* for 10 min. Supernatants were transferred to clean tubes for a second phenol:choloroform:isoamyl alcohol extraction. After centrifugation, supernatants were pooled into SnakeSkin dialysis tubing (Pierce) and dialyzed against 20 mM EGTA overnight at 4 °C. This large scale dialysis step proved to be very efficient in removing inorganic minerals and organic inhibitors. After dialysis, DNA was precipitated by adding 0.1 vol 3M sodium acetate and 1 vol isopropanol and stored at −20 °C for 2–4 h. Pellets were collected by centrifugation at 16,000 × *g* for 20 min at 8 °C, washed once in 70% ethanol, dried in a vacuum centrifuge, and resuspended in TE (10 mM Tris, 1 mM EDTA, pH 8). Typical yield was ~35 mg of DNA per g of carbonate chimney material.

Generation and Sequencing of V6 Amplicons. Archaeal and bacterial V6 amplicons were generated as previously described by Sogin et al. (2006) and Huber et al. (2007) and summarized here. PCR reactions used Platinum Taq HiFi polymerase (Invitrogen) to reduce errors introduced during amplification and involved the following cycling conditions: 94 °C for 2 min; 30 cycles of (94 °C for 30 s, 50 °C for 20 s, 72 °C for 1 min); and 72 °C for 2 min. A mixture of degenerate primers were used to maximize taxonomic coverage, as described by Huber et al. (2007). Amplicon concentrations were quantitated with a BioAnalyzer 2100 (Agilent Technologies) and normalized among samples before sequencing. Amplicons from each sample were attached to beads and sequenced with a 454 Life Sciences GS20 pyrosequencer according to previously published protocols (19, Sogin et al. [2006], Huber et al. [2007]). Archaeal data were also generated with a 454 Life Sciences FLX pyrosequencer because the number of archaeal sequences generated by the GS20 were highly variable among samples. Sequences generated by both machines were pooled together to improve OTU clustering robustness, but comparisons of archaeal diversity among samples considered only FLX data. Sequences were screened for quality as recommended by Huse et al. (20). Specifically, all sequences satisfying any of the following criteria were not considered for further analysis: those with one or more Ns, those without an exact match to one of the forward primers, or those shorter than 50 nts after removal of primers. Automated taxonomic assignments of V6 tag sequences were performed by the GAST process, which compares V6 tags to a reference database of V6 regions from full-length 16S rRNA clones of known taxonomy (1). GAST requires two-thirds of the sequences of a given taxonomy to match the query tag sequence to make an assignment. If no taxonomic category fulfills the two-thirds rule, it is reported as "Unassigned" (Tables S2 and S3). As the taxonomy of uncultured organisms is inconsistently reported in GenBank, GAST is frequently unable to reliably assign taxonomy to groups of organisms without cultured representatives (e.g., ANME-1 in Table S2).

Estimation of Pyrosequencing Error. Each of the three extremely dominant sequence types representing the main archaeal groups was one member of a large, unexpectedly diverse pool of mostly rare sequences (Fig. 3B). For example, the four chimney samples contained 1,242 different V6 sequence types that were 3% distant or less from the dominant sequence, representing nearly half of all 2,635 sequence types identified in this study. An additional 530 sequence types were between 3% and 10% distant from the dominant sequence. Only 63 sequence types were more than 10% distant to the dominant sequence (together, these 1,835 sequence types clustered into the 534 OTUs displayed in Fig. 3). Similar patterns were seen with sequences related to the ANME-1 and Marine Group I clones: 403 different V6 sequence types are 3% distant or less from the dominant ANME-1 sequence, and 125 sequence types are 3% distant or less from the dominant Marine Group I sequence. Although pyrosequencing error may have generated some of the variant sequences within clusters, pyrosequencing error alone cannot account for all of the observed diversity. If the variant sequences within each major cluster are compared to that cluster's dominant sequence, a nucleotide substitution rate of 0.18% is calculated for the LCMS cluster, 0.08% for the ANME-1 cluster, and 0.76% for the Marine Group I cluster. (The much higher substitution rate for the Marine Group I cluster is due to the relatively high abundance of two variant sequences compared to the dominant sequence.) These values are much higher than the substitution rate of 0.03% attributed to pyrosequencing error of quality-screened tags by Huse et al. . Therefore, some of the most abundant variant sequences are extremely unlikely to be generated by pyrosequencing error and most likely represent genuine diversity within the phylogenetic group.

Determination of Variability Caused by Amplicon Generation and Sequencing. Because the three young chimney samples share the same dominant LCMS V6 sequence type, nearly all community differences in the presence/absence of OTUs among samples involve rare sequences. It is possible that differences involving rare sequences could be a trivial result because of inherent variability of the technique. We tested this possibility by generating and sequencing replicate amplicon libraries from the same DNA preparation of sample 1 to test whether the rare OTU membership was reproduced. Because the replicate sequencing runs were performed months apart, with independent amplifications from template, and on different pyrosequencing machines (454 Life Sciences GS20 and FLX), we consider this a very conservative test of replication. The GS20 replicate yielded 17,425 tag sequences and 343 OTUs. The FLX replicate yielded 16,260 tag sequences and 342 OTUs. The GS20 OTUs were randomly resampled down to 16,260 sequences, reducing the number of OTUs to 286. The Bray-Curtis similarity between the OTUs of the sample 1 replicates was high (89%) because of the nearly identical relative abundances of the most common OTUs. As expected, incomplete sampling of the amplicon library caused differences in the presence/absence of the many rare OTUs so that the Jaccard similarity between replicates was just 50%. (When sequence types represented by only one tag ("singletons") among all samples were removed from analysis before normalization and clustering, the Jaccard similarity improved to 73%.) Because the similarity between replicates was higher than the similarity between sample 1 and the other samples, the differences among samples are greater than that expected from the technique itself. A remarkable exception is the archaeal community similarity between samples 2 and 3 (95% Bray-Curtis, 56% Jaccard). The similarity was much higher than the similarity

between sample 1 replicates, so the small differences between these samples may not reflect any natural variation. Therefore, the archaeal communities of samples 2 and 3 can be considered identical. It should be noted, however, that samples 2 and 3 were both sequenced on the same machine (FLX), whereas sample 1 replicates were sequenced on different machines, so the actual experimental error between samples sequenced on the same machine is probably much lower than that represented by the sample 1 replicates.

Comparison with Clone Libraries. The nearly full-length sequences of 16S rRNA clones to which V6 tag sequences were compared have been previously published (2, 21). Global alignment sequence similarities between V6 tags and the corresponding region of 16S rRNA clones were calculated with MatGat 22. Phylogenetic trees of 16S rRNA clones were constructed with TreePuzzle, Version 5.2 (23) using default options and exact parameter estimation. GenBank accession numbers for sequences in Fig. 3 tree, from top to bottom: M59133, FJ791573, M59140, AY817738, AM746096, NC_010085, FJ795512, U51469. GenBank accession numbers for sequences in Fig. 5 tree, from top to bottom: AF329082, AF016046, DQ270609, FJ792098, AF013974, DQ270608, DQ270607, FJ792484, AJ404732, AB166731, L40810.

1. Huse SM, et al. (2008) Exploring microbial diversity and taxonomy using SSU rRNA hypervariable tag sequencing. *PLoS Genet* 4:e1000255.
2. Brazelton WJ, Schrenk MO, Kelley DS, Baross JA (2006) Methane- and sulfur-metabolizing microbial communities dominate the Lost City hydrothermal field ecosystem. *Appl Environ Microbiol* 72:6257–6270.
3. Schrenk MO, Kelley DS, Bolton SA, Baross JA (2004) Low archaeal diversity linked to subseafloor geochemical processes at the Lost City Hydrothermal Field, Mid-Atlantic Ridge. *Environ Microbiol* 6:1086–1095.
4. Bradley AS, Hayes JM, Summons RE (2009) Extraordinary ^{13}C enrichment of diether lipids at the Lost City Hydrothermal Field indicates a carbon-limited ecosystem. *Geochim Cosmochim Acta* 73:102–118.
5. Ludwig KA, Kelley DS, Butterfield DA, Nelson BK, Fruh-Green G (2006) Formation and evolution of carbonate chimneys at the Lost City Hydrothermal Field. *Geochim Cosmochim Acta* 70:3625–3645.
6. Kelley DS, et al. (2005) A serpentinite-hosted ecosystem: the Lost City hydrothermal field. *Science* 307:1428–1434.
7. Proskurowski G, Lilley MD, Kelley DS, Olson EJ (2006) Low temperature volatile production at the Lost City Hydrothermal Field, evidence from a hydrogen stable isotope geothermometer. *Chem Geol* 229:331–343.
8. Proskurowski G, et al. (2008) Abiogenic hydrocarbon production at Lost City Hydrothermal Field. *Science* 319:604–607.
9. Früh-Green GL, et al. (2003) 30,000 Years of hydrothermal activity at the Lost City Vent Field. *Science* 301:495–498.
10. Edwards RL, Chen JH, Wasserburg GJ (1986/1987) U-238 U-234-TH-230-TH-232 systematics and the precise measurement of time over the past 500,000 years. *Earth Planet Sci Lett* 81:175–192.
11. Edwards RL, Chen JH, Ku TL, Wasserburg GJ (1987) Precise timing of the last interglacial period from mass-spectrometric determination of Th-230 in corals. *Science* 236:1547–1553.
12. Edwards RL, Gallup CD, Cheng H (2003) Uranium-series dating of marine and lacustrine carbonates. *Uranium-Series Geochemistry*, eds Bourdon S, Henderson G, Lundstrom CC, Turner SP (Mineralogical Society of America, New York), pp 363–405.
13. Shen CC, et al. (2003) Measurement of attogram quantities of 231Pa in dissolved and particulate fractions of seawater by isotope dilution thermal ionization mass spectroscopy. *Anal Chem* 75:1075–1079.
14. Chen JH, Edwards RL, Wasserburg GJ (1986) ^{238}U, ^{234}U, and ^{232}Th in seawater. *Earth Planet Sci Lett* 80:241–251.
15. Shen CC, et al. (2002) Uranium and thorium isotopic and concentration measurements by magnetic sector inductively coupled plasma mass spectrometry. *Chem Geol* 185: 165–178.
16. Cheng H, et al. (2000) The half-lives of uranium-234 and thorium-230. *Chem Geol* 169: 17–33.
17. Jaffey AH, Flynn KF, Glendenin LE, Bentley WC, Essling AM (1971) Precision measurement of half-lives and specific activities of U-235 and U-238. *Phys Rev* C4:1889–1906.
18. Barton HA, Taylor NM, Lubbers BR, Pemberton AC (2006) DNA extraction from low-biomass carbonate rock: An improved method with reduced contamination and the low-biomass contaminant database. *J Microbiol Methods* 66:21–31.
19. Margulies M, et al. (2005) Genome sequencing in microfabricated high-density picolitre reactors. *Nature* 437:376–380.
20. Huse SM, Huber JA, Morrison HG, Sogin ML, Welch DM (2007) Accuracy and quality of massively parallel DNA pyrosequencing. *Genome Biol* 8:R143. **Q:6**
21. Brazelton WJ, Baross JA (2009) Abundant transposases encoded by the metagenome of a hydrothermal chimney biofilm. *ISME J* 3:1420–1424.
22. Campanella JJ, Bitincka L, Smalley J (2003) MatGAT: An application that generates similarity/identity matrices using protein or DNA sequences. *BMC Bioinformatics* 4:29. **Q:7**
23. Schmidt HA, Strimmer K, Vingron M, von Haeseler A (2002) TREE-PUZZLE: Maximum likelihood phylogenetic analysis using quartets and parallel computing. *Bioinformatics* 18:502–504.

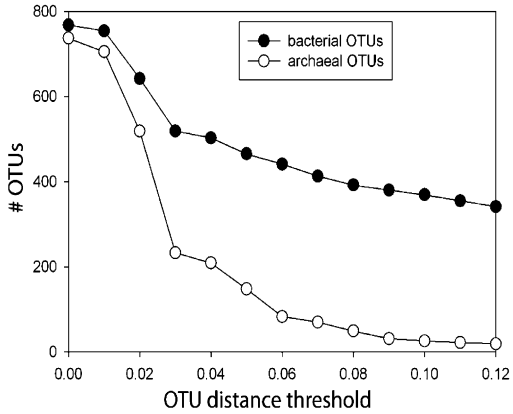

Fig. S1. Archaeal diversity is much lower than bacterial diversity at higher genetic distances. Number of archaeal and bacterial operational taxonomic units (OTUs) clustered at different pairwise distance thresholds are plotted for sample 2. At small distances, similar numbers of archaeal and bacterial OTUs were discovered. At large distances, very few archaeal OTUs were discovered, indicating very low diversity at high taxonomic levels (e.g., order, class, phylum).

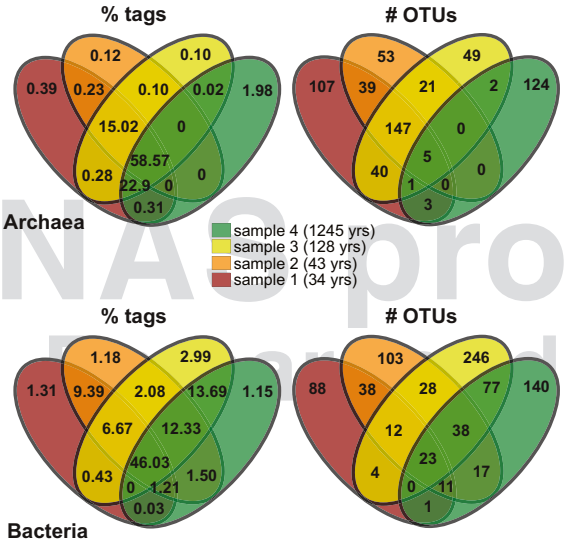

Fig. S2. Venn diagrams of archaeal and bacterial OTUs clustered with a 3% distance threshold showing the percentage of all tag sequences and the numbers of OTUs shared by the four chimney samples.

Archaeal V6 tag community similarities between samples

Bray-Curtis similarity	128 yrs	43 yrs	34 yrs
sample 4 (1245 yrs)	0.2	0.1	0.2
sample 3 (128 yrs)		95	87
sample 2 (43 yrs)			85
sample 1 (34 yrs)			

Jaccard similarity	128 yrs	43 yrs	34 yrs
sample 4 (1245 yrs)	1.9	1.1	1.5
sample 3 (128 yrs)		56	48
sample 2 (43 yrs)			50
sample 1 (34 yrs)			

Bacterial V6 tag community similarities between samples

Bray-Curtis similarity	128 yrs	43 yrs	34 yrs
sample 4 (1245 yrs)	36.1	37.7	12.1
sample 3 (128 yrs)		17.8	6.5
sample 2 (43 yrs)			45.0
sample 1 (34 yrs)			

Jaccard similarity	128 yrs	43 yrs	34 yrs
sample 4 (1245 yrs)	23.0	16.7	8.8
sample 3 (128 yrs)		17.4	8.3
sample 2 (43 yrs)			23.6
sample 1 (34 yrs)			

Fig. S3. Pairwise whole archaeal and bacterial community similarities between samples considering numbers of tag sequences in each OTU (Bray-Curtis) and considering only the presence/absence of each OTU (Jaccard).

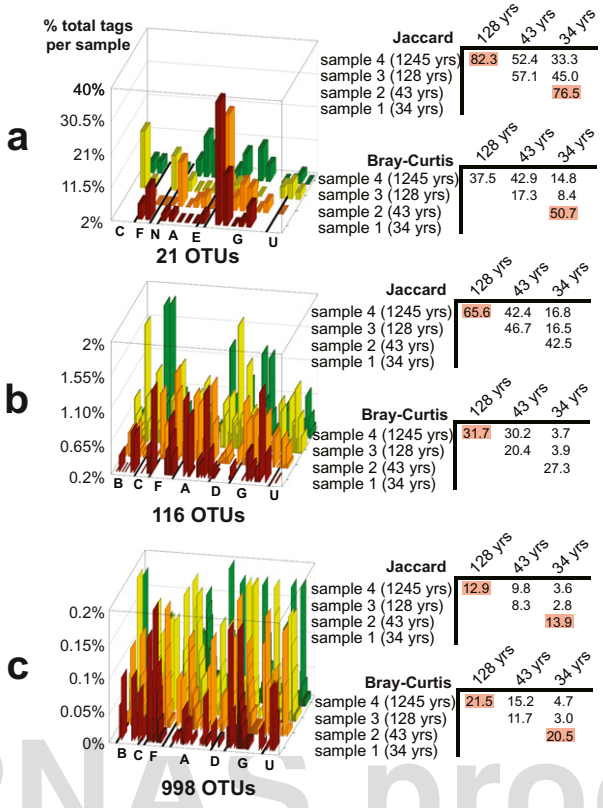

Fig. S4. Relative abundance of each bacterial OTU (clustered with a 3% distance threshold) in each of the four chimney samples and the resulting pairwise whole bacterial community similarities between samples. OTUs occurring at different relative abundance scales are displayed separately: (*A*) OTUs containing >2% of at least one sample's total tag sequences (*B*) OTUs containing 0.2% and 2% of a sample's total tag sequences (c) OTUs containing fewer than 0.2% of all samples' total tag sequences. Community similarities between samples remain fairly constant regardless of whether abundant or very rare OTUs are examined. The highest community similarities are typically between the two youngest samples and the two oldest samples (highlighted in red when they represent the two highest similarity values). OTUs are labeled according to their taxonomic assignment by GAST (1). A, Alphaproteobacteria; B, *Bacteroides*; C, Chloroflexus; D, Deltaproteobacteria; E, Epsilonproteobacteria; F, Firmicutes; G, Gammaproteobacteria; N, Nitrospira; U, Unassigned.

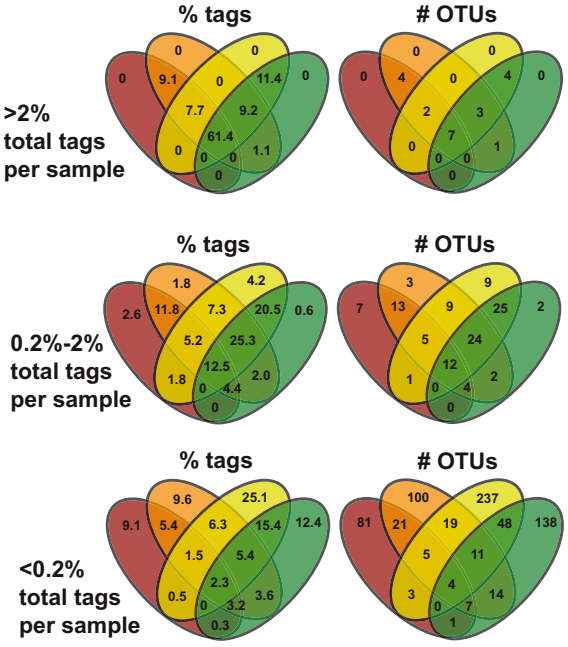

Fig. S5. Venn diagrams of bacterial OTUs (clustered with a 3% distance threshold) showing the percentage of all tag sequences and the numbers of OTUs shared by the four chimney samples. Separate Venn diagrams are shown for each of the relative abundance scales shown in Fig. S4.

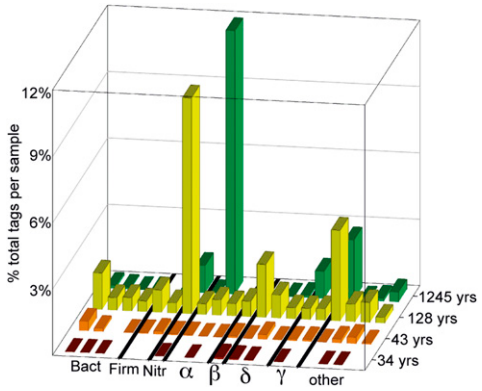

Fig. S6. Examples of OTUs that are dominant in old chimney samples and present but rare in young chimney samples. OTUs are labeled acccording to their taxonomic assignment. α, Alphaproteobacteria; β, Betaproteobacteria; Bact, *Bacteroides*; γ, Gammaproteobacteria; δ, Deltaproteobacteria; Firm, Firmicutes; Nitr, Nitrospira.

Table S1. Sequencing depth (as number of V6 tag sequences), observed number of OTUs (operational taxonomic units), richness estimators (ACE and Chao1), and Simpson's Reciprocal Index of diversity for all archaeal and bacterial OTUs in this study

	Archaea	Bacteria
V6 tag sequences	167,031	43,027
Unique sequence types	2,635 (1,163)	2,082
OTUs (3% distance)	817 (444)	1,135
ACE (3% distance)	980–1,024 (543–642)	2,203–2,362
Chao1 (3% distance)	943–1078 (524–641)	1,692–2,048
Simpson's Reciprocal Index (3% distance)	2.3 (2.3)	12.5
OTUs (10% distance)	116 (81)	653
ACE (10% distance)	142–191 (85–111)	1,215–1,294
Chao1 (10% distance)	130–246 (83–124)	922–1189
Simpson's Reciprocal Index (10% distance)	2.04 (2.04)	11.1

Values in parentheses are derived from randomly resampling the 167,031 archaeal tags down to 43,027 tags to compare archaeal diversity with bacterial diversity at equal sequencing efforts. The 167,031 archaeal tags includes 139,086 tags from the 454 Life Sciences FLX pyrosequencer and 27,945 tags from the 454 Life Sciences GS20 pyrosequencer.

Table S2. Numbers of archaeal tag sequences and OTUs clustered with a 3% distance threshold for the most frequently detected phyla, classes, and orders

			Sample 1 (34 yr)		Sample 2 (43 yr)		Sample 3 (128 yr)		Sample 4 (1,245 yr)	
Phylum	Class	Order	Tags	OTUs	Tags	OTUs	Tags	OTUs	Tags	OTUs
Crenarchaeota	MBGA	Unassigned	3	2	0	0	0	0	0	0
Crenarchaeota	MGI	Unassigned	5	3	0	0	0	0	0	0
Crenarchaeota	Thermoprotei	Unassigned	45	11	0	0	3	1	2	1
Crenarchaeota	Unassigned	Unassigned	259	27	0	0	10	5	7	4
Euryarchaeota	Methanomicrobia	Methanosarcinales	14,689	281	16,258	264	16,199	256	12	4
Euryarchaeota	Methanomicrobia	Methanosaetaceae	0	0	0	0	0	0	265	5
Euryarchaeota	Misc.		4	1	0	0	0	0	2	1
Euryarchaeota	Unassigned	Unassigned	53	15	0	0	2	1	15,935	116
Korarchaeota	Unassigned	Unassigned	2	1	0	0	0	0	0	0
Unassigned	Unassigned	Unassigned	1020	1	2	1	46	1	37	4
Archaea total			16,260	342	16,260	265	16,260	265	16,260	135

Q:8 Taxonomies were assigned with the GAST algorithm (1). Numbers of tag sequences have been normalized down to a total of 16,260 sequences per sample by random resampling after OTU clustering. Prenormalized total numbers of tag sequences were 16,260 (sample
Q:9 1); 32,345 (sample 2); 25,471 (sample 3); and 21,983 (sample 4). Most of the OTUs labeled 'LCMS' in Fig. 3 were assigned to order Methanosarcinales; most ANME-1 OTUs were assigned to Euryarchaeota unassigned; and most MGI OTUs were assigned to "Crenarchaeota unassigned" or "unassigned."

Table S3. Numbers of bacterial tag sequences and OTUs clustered with a 3% distance threshold for the most frequently detected phyla, classes, and orders

			Sample 1 (34 yr)		Sample 2 (43 yr)		Sample 3 (128 yr)		Sample 4 (1,245 yr)	
Phylum	Class	Order	Tags	OTUs	Tags	OTUs	Tags	OTUs	Tags	OTUs
Acidobacteria	Acidobacteria	Acidobacteriales	0	0	0	0	10	7	3	2
Acidobacteria	Unassigned	Unassigned	0	0	0	0	1	1	0	0
Actinobacteria	Actinobactera	Misc.	0	0	2	2	12	5	23	9
Actinobacteria	Unassigned	Unassigned	0	0	0	0	3	1	14	2
Bacteroidetes	Bacteroidia	Bacteroidales	0	0	0	0	3	1	1	1
Bacteroidetes	Flavobacteria	Flavobacteriales	27	7	103	18	301	37	40	10
Bacteroidetes	Sphingobacteria	Sphingobacteriales	42	4	29	8	39	21	11	9
Bacteroidetes	Unassigned	Unassigned	36	2	11	4	48	12	3	1
BRC1	Unassigned	Unassigned	0	0	0	0	89	5	163	9
Chloroflexi	Anaerolineae	Unassigned	2	1	0	0	0	0	0	0
Chloroflexi	Caldilineae	Caldilineales	1	1	3	1	11	1	1	1
Chloroflexi	Dehalococcoidetes	Unassigned	0	0	0	0	1,083	17	518	8
Deferribacteres	Deferribacteres	Deferribacterales	5	1	0	0	7	2	1	1
Deferribacteres	Unassigned	Unassigned	0	0	0	0	1	1	0	0
Deinococcus-Thermus	Deinococci	Misc.	31	4	0	0	0	0	0	0
Firmicutes	Bacilli	Misc.	0	0	1	1	2	1	0	0
Firmicutes	Clostridia	Misc.	1,073	42	426	31	228	21	57	9
Nitrospira	Nitrospira	Nitrospirales	0	0	3	1	601	8	83	3
OD1	Unassigned	Unassigned	0	0	8	2	62	10	10	5
Proteobacteria	Alphaproteobacteria	Misc.	15	3	24	10	14	9	9	7
Proteobacteria	Alphaproteobacteria	Rhizobiales	121	3	15	6	64	6	45	13
Proteobacteria	Alphaproteobacteria	Rhodobacterales	273	19	1294	40	545	39	2146	50
Proteobacteria	Alphaproteobacteria	Unassigned	102	9	108	7	149	25	140	16
Proteobacteria	Betaproteobacteria	Burkholderiales	15	3	11	5	72	6	13	7
Proteobacteria	Betaproteobacteria	Misc.	0	0	3	1	6	3	0	0
Proteobacteria	Deltaproteobacteria	Desulfobacterales	5	2	52	9	379	30	96	13
Proteobacteria	Deltaproteobacteria	Desulfovibrionales	15	5	3	3	2	2	1	1
Proteobacteria	Deltaproteobacteria	Misc.	0	0	14	6	18	11	14	9
Proteobacteria	Epsilonproteobacteria	Campylobacterales	158	9	29	9	36	11	21	4
Proteobacteria	Epsilonproteobacteria	Nautiliales	0	0	0	0	1	1	0	0
Proteobacteria	Gammaproteobacteria	Methylococcales	0	0	54	3	233	7	221	6
Proteobacteria	Gammaproteobacteria	Thiotrichales	3,483	42	3,122	56	371	21	1,429	30
Proteobacteria	Gammaproteobacteria	Misc.	114	10	153	21	459	42	192	32
Proteobacteria	Unassigned	Unassigned	2	2	52	11	325	14	182	15
Tenericutes	Mollicutes	Acholeplasmatales	0	0	1	1	35	4	5	2
Thermomicrobia	Unassigned	Unassigned	2	1	3	1	23	1	2	2
Misc. assigned*			42	6	7	7	63	23	21	11
Unassigned			3	1	36	6	271	22	102	19
Bacteria total			5,567	177	5,567	270	5,567	428	5,567	307

Taxonomies were assigned with the GAST algorithm (1). Numbers of tag sequences have been normalized down to a total of 5,567 sequences per sample by random resampling after OTU clustering. Prenormalized total numbers of tag sequences were 21,582 (sample 1); 5,567 (sample 2); 7,162 (sample 3); and 8,716 (sample 4). All of the *Thiomicrospira* sequences in Fig. 6 are included under Thiotrichales here. Most of the "misc" Clostridia sequences have high sequence similarity to previously published *Desulfotomaculum*-like clones (2).

*Misc. assigned includes: Chlamydiae, Chlorobi, Cyanobacteria, Fibrobacteres, Fusobacteria, Gemmatimonadetes, Lentisphaerae, Planctomycetes, Spirochaetes, Thermotogae, TM7, and Verrucomicrobia

Table S4. Previously published microbiological and biochemical characteristics of the four carbonate chimney samples

	Cells·g^{-1} dry weight*	Archaea†	Bacteria†	LCMS†	Total organic carbon, %	$\delta^{13}C_{toc}$, ‰ vs. VPDB
Sample 1 (3,881–1,408)	2.0×10^8	25	14	18	ND	ND
Sample 2 (3,869–1,404)	$1{,}200 \times 10^8$	41	8	32	0.20	−7.8
Sample 3 (3,869–1,443)	$1{,}600 \times 10^8$	38	10	21	ND	ND
Sample 4 (3,876–1,133)	1.6×10^8	24	19	12	0.15	−16.3

Q:11 Cell densities and proportions of phylogenetic groups are from Schrenk et al. (3) and M. Schrenk (doctoral dissertation, 2005). Organic carbon concentrations and isotopic measurements are from Bradley et al. (4).

*Determined by DAPI staining.

†Percentage of DAPI-stained cells detected by FISH probe specific to each group.

AUTHOR QUERIES

AUTHOR PLEASE ANSWER ALL QUERIES

Q: 1_Please note that Chen and Wasserberg (1981), as well as several other authors cited by name, are not in the SI reference list. Please add to reference list and renumber all remaining references and citations accordingly or delete mention from text.

Q: 2_PNAS no longer allows references to unsupported data. For reference XX, please (a) provide the data as Supporting Information, (b) provide an "in press" reference if the article has been accepted for publication, or (c) remove the reference from the list, as well as its corresponding statement in the text, and renumber all subsequent references.

Q: 3_Please verify that 3M refers to the manufacturer rather than indicating a volume of 3 M.

Q: 4_Please note that Sogin et al. and Huber et al. (2007), each mentioned at least twice in this paragraph, are not in the *SI* reference list. Please add to list or delete from *SI* text.

Q: 5_Please advise whether this citation of Huse et al. refers to reference 1 or reference 20 in the SI reference list.

Q: 6_Reference has only first page number. Please provide the last page number if article is longer than one page. (in reference 12 "Huse, Huber, Morrison, Sogin, Welch, 2007").

Q: 7_Reference has only first page number. Please provide the last page number if article is longer than one page. (in reference 5 "Campanella, Bitincka, Smalley, 2003").

Q: 8_Please note that all references in *SI* have been renumbered according to order of citation in *SI*.

Q: 9_No figure matches the in-text citation "Fig. 3". Please supply a legend and figure or delete the citation.

Q: 10_No figure matches the in-text citation "Fig. 6". Please supply a legend and figure or delete the citation.

Q: 11_Please move information on doctoral dissertation to a footnote and include title as if this were a regular reference.